H. Kazerooni
Ryan Steger
Lihua Huang

Department of Mechanical Engineering
University of California
Berkeley, California 94720 USA
exo@berkeley.edu

Hybrid Control of the Berkeley Lower Extremity Exoskeleton (BLEEX)

Abstract

The Berkeley Lower Extremity Exoskeleton is the first functional energetically autonomous load carrying human exoskeleton and was demonstrated at U.C. Berkeley, walking at the average speed of 0.9 m/s (2 mph) while carrying a 34 kg (75 lb) payload. The original published controller, called the BLEEX Sensitivity Amplification Controller, was based on positive feedback and was designed to increase the closed loop system sensitivity to its wearer's forces and torques without any direct measurement from the wearer. This controller was successful at allowing natural and unobstructed load support for the pilot. This article presents an improved control scheme we call "hybrid" BLEEX control that adds robustness to changing BLEEX backpack payload. The walking gait cycle is divided into stance control and swing control phases. Position control is used for the BLEEX stance leg (including the torso and backpack) and a sensitivity amplification controller is used for the swing leg. The controller is also designed to smoothly transition between these two schemes as the pilot walks. With hybrid control, the controller does not require a good model of the BLEEX torso and payload, which is difficult to obtain and subject to change as payload is added and removed. As a tradeoff, the position control used in this method requires the human to wear seven inclinometers to measure human limb and torso angles. These additional sensors require careful design to securely fasten them to the human and increase the time to don and doff BLEEX.

KEY WORDS—BLEEX, exoskeleton, human-machine, wearable robotics, control, load support, sensitivity amplification, master-slave, hybrid control

1. Introduction

BLEEX was first unveiled in 2004, at U.C. Berkeley's Human Engineering and Robotics Laboratory (Figure 1). The primary

objective of this project is to develop fundamental technologies that augment human strength and endurance during locomotion. The first field-operational lower extremity exoskeleton (commonly referred to as BLEEX) is comprised of two powered anthropomorphic legs, a power unit, and a backpack-like frame on which a variety of heavy loads can be mounted. This system provides its pilot (i.e., the wearer) with the ability to carry significant loads on his/her back with minimal effort over any type of terrain. BLEEX allows the pilot to comfortably squat, bend, swing from side to side, twist, and walk on ascending and descending slopes, while also offering the ability to step over and under obstructions while carrying equipment and supplies. The overall concept of this lower extremity exoskeleton is that the human provides an intelligent control system for the exoskeleton while the exoskeleton actuators provide most of the strength necessary for walking.

BLEEX has numerous potential applications; it can provide soldiers, disaster relief workers, wildfire fighters, and other emergency personnel with the ability to carry heavy loads such as food, rescue equipment, first-aid supplies, communications gear, and weaponry, without the strain typically associated with demanding labor.

The original control algorithm was designed to increase the closed loop system sensitivity to its wearer's forces and torques without any measurement from the wearer. As an alternative, this article presents the hybrid BLEEX control scheme. Position control is used for the stance leg (including torso) and a sensitivity amplification controller is used for the swing leg.

2. Background

In the early 1960s, the Defense Department expressed interest in the development of a man-amplifier: a "powered suit of armor" which would augment soldiers' lifting and carrying capabilities. In 1962, the Air Force had the Cornell Aeronautical Laboratory study the feasibility of using a master-slave robotic system as a man-amplifier. In later work, Cornell determined that an exoskeleton, an external structure in the shape

561

Payload and power supply

BLEEX spine and harness

Control computer

Hydraulic actuators

Control network node
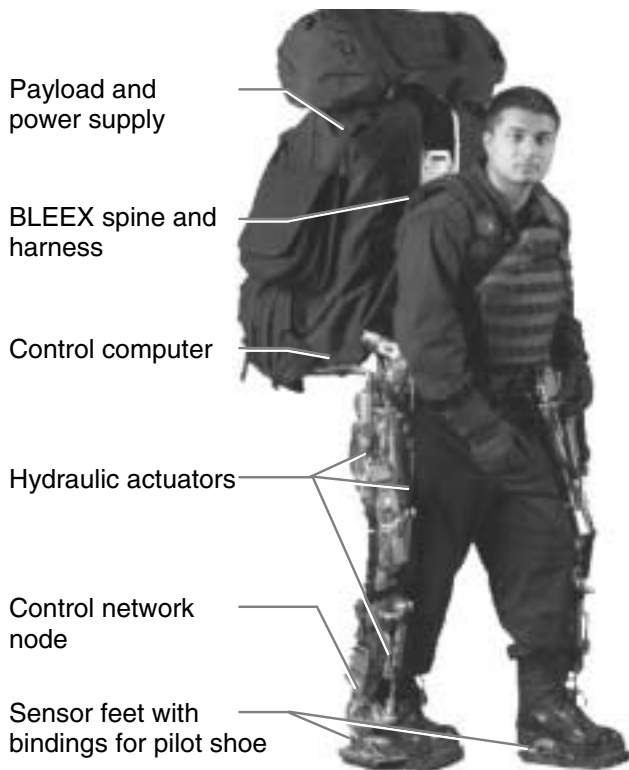
Sensor feet with bindings for pilot shoe

Fig. 1. Berkeley Lower Extremity Exoskeleton (BLEEX) and pilot.

of the human body that has far fewer degrees of freedom than a human, could accomplish most desired tasks (Mizen 1965). From 1960 to 1971, General Electric developed and tested a prototype man-amplifier, a master-slave system called the Hardiman (Mosher 1960, 1967; General Electric Co. 1966, 1968; Groshaw 1969; Makinson 1971). The Hardiman was a set of overlapping exoskeletons worn by a human operator. The outer exoskeleton (the slave) followed the motions of the inner exoskeleton (the master), which followed the motions of the human operator. All these studies found that duplicating all human motions and using master-slave systems were not practical. Additionally, difficulties in human sensing and system complexity kept it from walking.

Several exoskeletons were developed at the University of Belgrade in the 60s and 70s to aid paraplegics (Vukobratovic, Ciric, and Hristic 1972; Hristic and Vukobratovic 1973). Although these early devices were limited to predefined motions and had limited success, balancing algorithms developed for them are still used in many bipedal robots (Hirai et al. 1998; Colombo, Jorg, and Dietz 2000). The "RoboKnee" is a powered knee brace that functions in parallel to the wearer's knee and transfers load to the wearer's ankle (not to the ground; Pratt et al. 2004). "HAL" is an orthosis, connected to the thighs and shanks, that moves a patient's legs as a function

of EMG signals measured from the wearer (Kawamoto and Sankai 2002; Kawamoto, Kanbe, and Sankai 2003).

In our research work at Berkeley, we have separated the technology associated with human power augmentation into lower extremity exoskeletons and upper extremity exoskeletons. The reason for this was two-fold; firstly, we could envision a great many applications for either a stand-alone lower or upper extremity exoskeleton in the immediate future. Secondly, and more importantly for the division, is that the exoskeletons are in their early stages, and further research still needs to be conducted to ensure that the upper extremity exoskeleton and lower extremity exoskeleton can function well independently before we can venture an attempt to integrate them. With this in mind, we proceeded with the designs of the lower and upper extremity exoskeleton separately, with little concern for the development of an integrated exoskeleton. We will first give a summary of the upper extremity exoskeleton efforts at Berkeley and then we will proceed with the description of the BLEEX project.

In the mid-1980s, we initiated several research projects on upper extremity exoskeleton systems, billed as "human extenders" (Kazerooni 1990, 1995, 1996; Kazerooni and Mahoney 1991; Kazerooni and Guo 1993; Kazerooni and Her 1994; Kazerooni and Snyder 1995). The main function of an upper extremity exoskeleton is human power augmentation for manipulation of heavy and bulky objects. These systems, which are also known as assist devices or human power extenders, can simulate forces on a worker's arms and torso. These forces differ from, and are usually much less than the forces needed to maneuver a load. When a worker uses an upper extremity exoskeleton to move a load, the device bears the bulk of the weight by itself, while transferring to the user as a natural feedback, a scaled-down value of the load's actual weight. For example, for every 40 pounds of weight from an object, a worker might support only 4 pounds while the device supports the remaining 36 pounds. In this fashion, the worker can still sense the load's weight and judge his/her movements accordingly, but the force he/she feels is much smaller than what he/she would feel without the device. In another example, suppose the worker uses the device to maneuver a large, rigid, and bulky object, such as an exhaust pipe. The device will convey the force to the worker as if it was a light, single-point mass. This limits the cross-coupled and centrifugal forces that increase the difficulty of maneuvering a rigid body and can sometimes produce injurious forces on the wrist. In a third example, suppose a worker uses the device to handle a powered torque wrench. The device will decrease and filter the forces transferred from the wrench to the worker's arm so the worker feels the low-frequency components of the wrench's vibratory forces instead of the high-frequency components that produce fatigue.

The Berkeley Lower Extremity Exoskeleton (BLEEX) is not an orthosis or a brace; unlike the above systems it is designed to carry a heavy load by transferring the load weight

to the ground (not to the wearer). BLEEX introduced four new features. First, a novel control architecture was developed that controls the exoskeleton through measurements of the exoskeleton itself (Kazerooni et al. 2005). This eliminated problematic human induced instability (Kazerooni et al. 2005) due to sensing the human force. Second, a series of high specific power and specific energy power supplies were developed that were small enough to make BLEEX a true field-operational system (McGee, Raade, and Kazerooni 2004; Raade and Kazerooni 2004; Amundsen et al. 2005). Third, a body LAN (Local Area Network) with a special communication protocol and hardware was developed to simplify and reduce the cabling task of all the sensors and actuators needed for exoskeleton control (Kim, Anwar, and Kazerooni 2004; Kim, and Kazerooni 2004). Finally, a flexible and versatile mechanical architecture was chosen to decrease complexity and power consumption (Chu, Kazerooni, and Zoss 2005; Zoss and Kazerooni 2005). This paper gives an overview of the biomimetic design of this architecture.

3. Mechanical Description

For BLEEX, we choose a pseudo-anthropomorphic design. The exoskeleton has a rigid spine that serves as a payload attachment point and an exoskeleton-to-human attachment point through a compliant harness. Three-segment legs, analogous to the human's thigh, shank, and foot, run parallel to the human's leg segments when the device is worn. Single DOF revolute joints connect each leg segment and between the thigh and spine on each side. A servo-valve-controlled hydraulic cylinder spans each segment pair to provide an active torque source at the hip (flexion and abduction), knee, and ankle of each exoskeleton leg.

As shown in Figure 2, additional unpowered passive degrees of freedom exist at the hip and ankle and include experimentally chosen passive impedances (created by steel springs and elastomers). BLEEX is considered pseudo-anthropomorphic because we have not included every human degree of freedom or attempted to match the joint behavior of the human exactly (e.g., the human knee uses a combination of rotation and sliding but the exoskeleton has a pure rotary joint). We determined, through extensive testing of unpowered mockups both in our lab and independently at the U.S. Army Natick Soldier Testing Center, that the kinematics of the configuration shown in Figure 2 allow for unrestricted walking, running, kneeling, and crawling, and therefore is sufficient for this design. In the hybrid control experiment, only the sagittal plane is considered and hip abduction-adduction joints are not powered.

The pilot and BLEEX have mechanical connections at the torso and the feet; everywhere else the pilot and BLEEX have compliant or periodic contact (Figures 3 and 4). The connection at the torso is made using a custom vest. One of the

Fig. 2. BLEEX mechanical structure and degrees of freedom.

essential objectives in the design of these custom vests was to allow the distribution of the forces between BLEEX and the pilot, thereby preventing abrasion. The vest is made of several hard surfaces that are compliantly connected to each other using thick fabric. The adjustment mechanisms in the vest allow for a snug fit to the pilot. The vest includes rigid plates (with hole patterns) on the back for connection to the BLEEX torso (Zoss and Kazerooni 2005).

Because the exoskeleton kinematics are close to human kinematics, appropriate ranges of motion for each degree of freedom could be approximated from human physiological data (Woodson, Tillman, and Tillman 1992). Slight human-machine kinematic differences are tolerated for design simplicity. These differences are not uncomfortable for the human because the human and the machine are only rigidly connected at the extremities of the exoskeleton (feet and torso). Any other rigid connections would lead to large forces imposed on the operator due to the kinematic differences. However, compliant connections along the leg are tolerable as long as they allow relative motion between the human and machine. Because the inertias and masses of the exoskeleton leg segments were similar to the corresponding human limbs, the desired joint torques for the exoskeleton were estimated using hu-

Front   Side

Fig. 3. The pilot vests in this figure and in Figure 1 are designed to uniformly distribute the BLEEX-pilot force on the pilot's upper body (note that the BLEEX power supply is not attached in the "side" image).
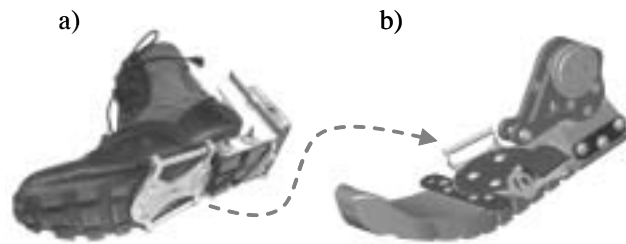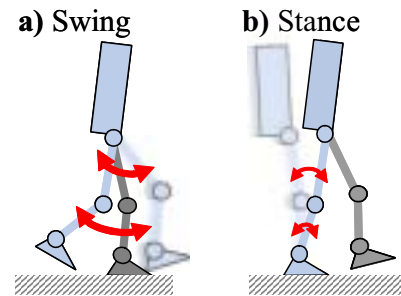

a) Swing   **b)** Stance

Fig. 5. BLEEX single leg gait phase distinctions: a) swing leg: large angle motion, low torques, no payload support; b) stance leg: small angle motion, large torques, full payload support.

a)   b)

Fig. 4. Foot attachment mechanism showing a) the cleat attached to the pilot boot and b) the mating cleat on the BLEEX foot.

man Clinical Gait Analysis (CGA) data (Winter 1990; Riener, Rabuffetti, and Frigo 2002; Kirtley 2005; Linskell 2005).

4. Hybrid Control of BLEEX

Looking at the entire walking gait cycle, the swing leg undergoes large motions but it is only supporting its own weight—it needs relatively small torques and high bandwidth. The stance leg goes through a small motion but supports the entire torso and payload—it needs large torques and relatively low bandwidth. Based on these observations, hybrid control is put forward. For a single leg, the walking gait cycle is divided into a load support stance phase and an unloaded swing phase (Figure 5). With hybrid control, position control is applied to the leg when it is in the stance phase and a positive feedback based sensitivity amplification controller is applied to the swing leg. At any instant, for any powered joint, only one control method is determining the control signal.

For the stance leg (i.e., the leg that is on ground), position control is used to servo BLEEX joint angles to track the human's joint angles. Since the BLEEX torso weight is car-

ried by the stance leg, there is no need to know the mass and center of gravity (CG) properties of the torso. For the swing leg, a positive feedback sensitivity amplification controller, identical to the one presented in Kazerooni et al. (2005), is used. Provided the controller has a precise dynamic model of the BLEEX structure, this controller allows BLEEX to track rapid human limb motions without impeding the human. Thus, robust stability (position controlled stance leg) and a high sensitivity to the human forces and torques (sensitivity amplification controlled swing leg) can be maintained simultaneously.

4.1. Stance Phase: Position Control

Stance phase position control of the exoskeleton is motivated through a 1 DOF example shown in Figure 6. This figure schematically depicts the master (a human leg) interacting with the slave (a 1 DOF exoskeleton leg in the stance configuration). The exoskeleton leg is shown as a rigid link pivoting about an ankle joint and powered by a single actuator that generates a torque T_{act}. The interaction between human leg and the exoskeleton leg in this example is interpreted as a spring-damper connection. This interaction generates an equivalent torque d about pivot joint.

Figure 7 shows the control block diagram of Figure 6, where G represents the transfer function from the actuator torque T_{act} to the exoskeleton angular velocity v. C is the exoskeleton controller. The sensitivity transfer function, S (upper case), maps the equivalent interaction torque d onto the exoskeleton angular velocity v. The human–machine interaction torque, d, is a function of H, the interaction dynamics between the pilot and the exoskeleton, and the kinematics of the pilot limb and exoskeleton leg (e.g., velocity, position, or a combination thereof). For stance control, as will be explained in following paragraphs, the connection between the human and exoskeleton needs to be compliant. θ_h and θ_{exo} (i.e., θ_e)
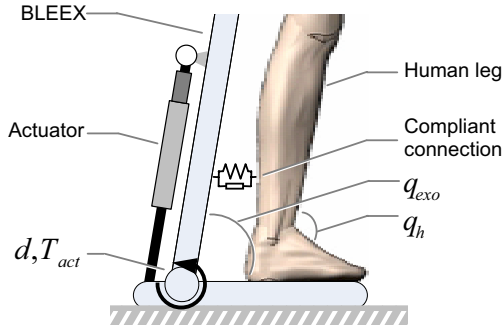
Fig. 6. 1-DOF master-slave schematic with a representation of the compliant human leg connection to BLEEX.
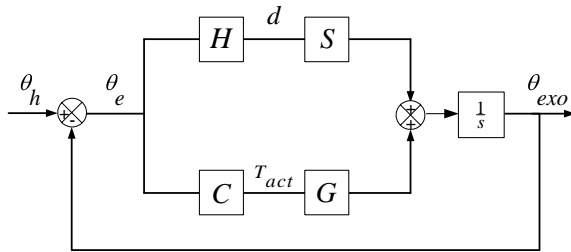

Fig. 7. Block diagram of 1 DOF position control.

are different and this difference is used as the input to our controller. Lower case s is used to represent the Laplace operator.

The goal is to design a controller such that small θ_e can be achieved, i.e., BLEEX can track the human's motion. Notice that $d = H\theta_e$; small θ_e actually means small d. Therefore, BLEEX can track the human's motion without the human feeling an interaction force. The design specification is given by:

$$\left| \frac{\theta_{exo}}{\theta_h} \right| = \left| \frac{SH + GC}{s + SH + GC} \right| \approx 1 \ \forall \omega \in (0, \omega_0) \qquad (1)$$

The controller is designed as a proportional controller by:

$$T_{act} = K(\theta_h - \theta_{exo}). \qquad (2)$$

To illustrate this scheme, 1 DOF master-slave position control is implemented on the left knee of BLEEX. To create a 1 DOF environment, BLEEX is put on a custom jig stand so that it is in jump mode (both feet are off the ground), and all the joint valves are closed except the left knee. The human then moves her shank randomly and BLEEX tries to follow it. Figure 8 shows the Bode plot of joint angle tracking. The data is collected from the BLEEX GUI, where the sampling

period is 25 msec. Figure 9 shows angle tracking of a sinusoidal reference signal generated in software for 0.2 Hz, 2 Hz, and 4 Hz motion. The tracking is good at the low frequencies that encompass normal human joint activity. The knee joint angle is defined as zero degrees when the thigh and shank are aligned in the sagittal plane. Relative to the thigh, if the shank is rotating counterclockwise, the knee angle is increasing in the positive direction. The controller used is a proportional controller. More advanced controllers can be used to achieve better tracking. However, as the following paragraphs will explain, the flexible contact between human and BLEEX means that perfect tracking is not necessary as long as BLEEX is supporting the load and the human is not experiencing any discomfort.

4.2. Implementation of Position Control

Master-slave position control is implemented for the entire stance leg, which is a multi-degree of freedom system. Here, the master trajectories are the human joint angles (hip, knee, and ankle) and the slaves are the corresponding BLEEX joint angles. A proportional controller is used on each joint to cause the BLEEX joint angles to track human joint angles.

The closed loop block diagram for each stance leg joint is shown in Figure 10; θ_{hi} is i^{th} human joint angle and θ_{exoi} is BLEEX i^{th} joint angle. The actuator dynamics do not appear in the closed loop block diagram explicitly. The torques exerted on BLEEX include equivalent human machine interaction torque T_{hmi} (corresponding to d in Figure 7), actuator torque T_{acti}, and gravity torque T_{gi}. In this control loop, θ_{hi} serves as desired value and θ_{exoi} as measured value. The goal of the proportional controller is to make the error between the two joint angles as small as possible. Our controller is designed as:

$$u_i = k_{pi}(\theta_{hi} - \theta_{exoi}), \qquad (3)$$

where u_i is the valve voltage for i^{th} joint. Comparing with Figure 7, human impedance H has been omitted in this block diagram. Also, human sensitivity S and BLEEX dynamics G are expressed in term of the BLEEX i^{th} stance joint.

BLEEX is a multi-degree freedom system and the exact dynamic model is correspondingly complicated. In addition, the human-BLEEX interface is not a linear spring-damper system and it is not easy to model. As is done in many complicated nonlinear systems (especially in bipedal robots), position control is used to reduce the importance of a precise system model. The optimum k_{pi} is obtained through experimentation. A benefit of using this controller is that the computation time is greatly reduced because the position control calculations for a three DOF stance leg are significantly simpler than the three DOF stance leg inverse dynamics computations used in sensitivity amplification controller.

The success of this simple control scheme owes much to the considerations made in the mechanical design. An important
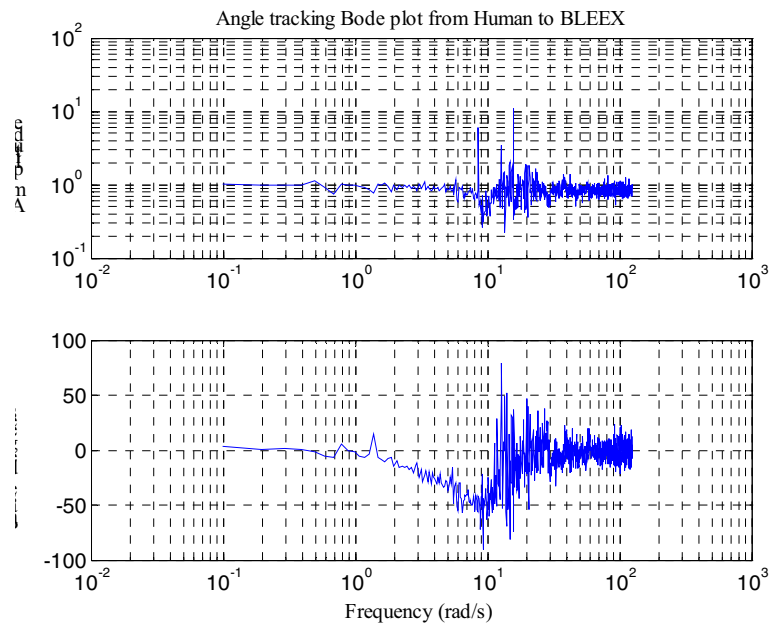
Fig. 8. Bode plot of experiment results from 1 DOF (knee joint) master-slave control joint angle tracking.
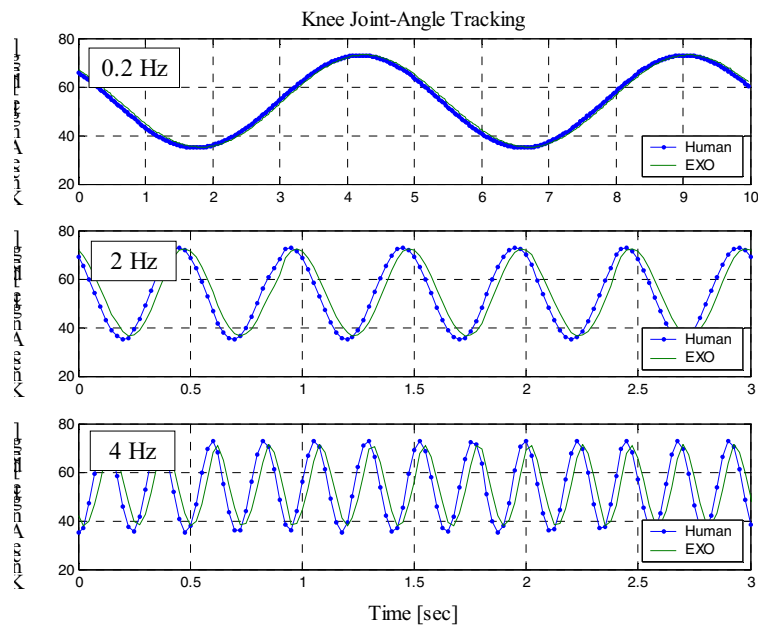

Fig. 9. Knee joint angle tracking results for master-slave control with a periodic reference signal scaled to match average walking gait cycle range of motion.
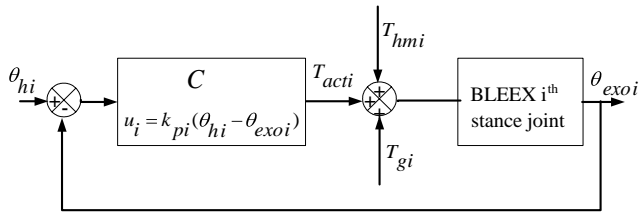
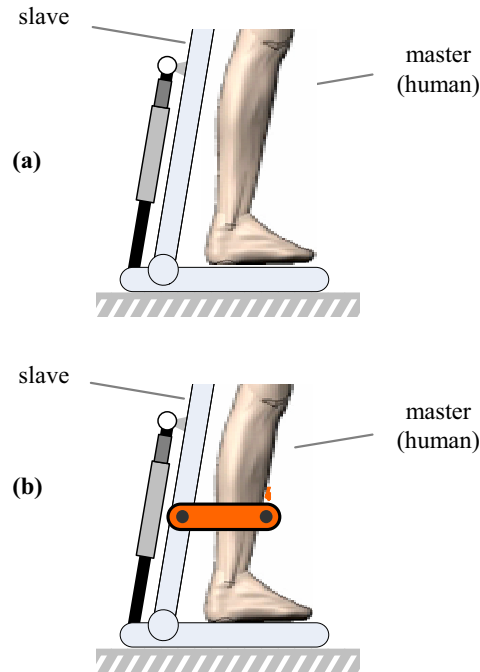Fig. 10. Position control block diagram for ith joint.

Fig. 11. 1-DOF mechanism master-slave conceptual representation with no physical connection between the human and machine (a); and with a rigid physical connection (b).

principle of BLEEX design is that it should not impede the wearer's movement. Applying this principle to position control, it means that if the human wants to move, they should be able to move to the desired position easily, thus creating a detectable BLEEX-human desired joint angle difference to servo. How easily the wearer can move relative to BLEEX depends on the connection between the human and BLEEX and the controller tracking.

A 1 DOF mechanism is shown in Figure 11 to illustrate how the contact between the master (human) and slave (BLEEX) influences the motion of the master. The foot is on ground and not moving, while the shank is rotating about the ankle. For Figure 11(a), there is no constraint between the master and slave. If the master wants to move, he/she simply moves to a new position. The position controller will cause the slave to follow the master without impeding the master's motion.

However, for the mechanism shown in Figure 11(b) the master and slave are bound together. If master wants to move, it needs to move not only itself, but also the slave. Since they are bound together, the joint angle error between the master and slave is zero and the output of the controller is zero. Thus, position control with a rigid connection between master and slave impedes the motion of the master.

As described earlier, the human and BLEEX are connected in two locations: the torso and foot. Similarly to Figure 11(b), if the human torso is rigidly connected with the BLEEX torso, and the human attempts to lean forward, backward, or squat without moving their foot, then the human will be unable to generate an angle difference with BLEEX joints and the position controller will impede the human's motion. Thus, a flexible harness on the torso is necessary.

The connection between BLEEX and the human is illustrated in Figure 12. The interface is illustrated as multiple spring-damper structures between BLEEX and the human. In reality, the foot attachment consists of a flexible binding and strap mechanism and the torso connection is a compliant backpack-like harness. There are no mechanical connections to the human on the shank and thigh, however the spring-damper structures in Figure 12 are shown as a representation of potential voluntary intermittent contact between the human and BLEEX. Relative to BLEEX, the torso connection gives the human freedom in both the horizontal and vertical direc-

tions. In addition, our foot fixture is designed in a way that the human can rotate her toe or heel 15 degrees relative to BLEEX foot. This semi-rigid foot connection is also useful in the toe-off and heel-strike stages of the gait cycle.

Beside the contact issue, another aspect that needs consideration is matching the geometry between the human and BLEEX. BLEEX is designed to adjust its thigh and shank length within a certain range (5–95% percentile U.S. Army Male; Zoss and Kazerooni 2005). Even so, the human link length and BLEEX link length are not guaranteed to be equal because of the discrete steps in the length adjustment mechanism. With master–slave control used on the stance leg, when the human squats, stands up, or leans back and forth, the length mismatch causes the distance between human and BLEEX torso to change. The relative position between the human and BLEEX is not important as long as this position difference does not cause BLEEX to exert an uncomfortable force on the human. When a flexible harness is used, the distance change between the human and BLEEX torso in the horizontal direction is not problematic as long as the BLEEX CG is within the area of the BLEEX foot and the harness is not too tight. In the vertical direction, to ensure the BLEEX harness is not too tight in any particular human posture we need to loosen the harness so that when the human stands straight, this harness can be lifted off their shoulders by approximately 3–6 cm.
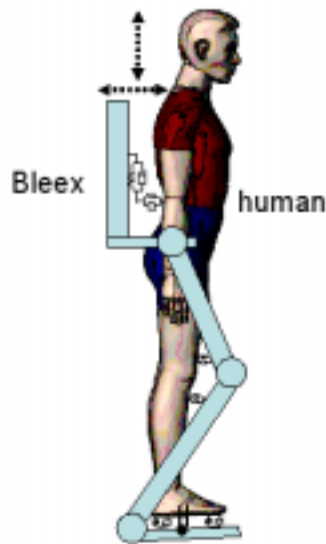
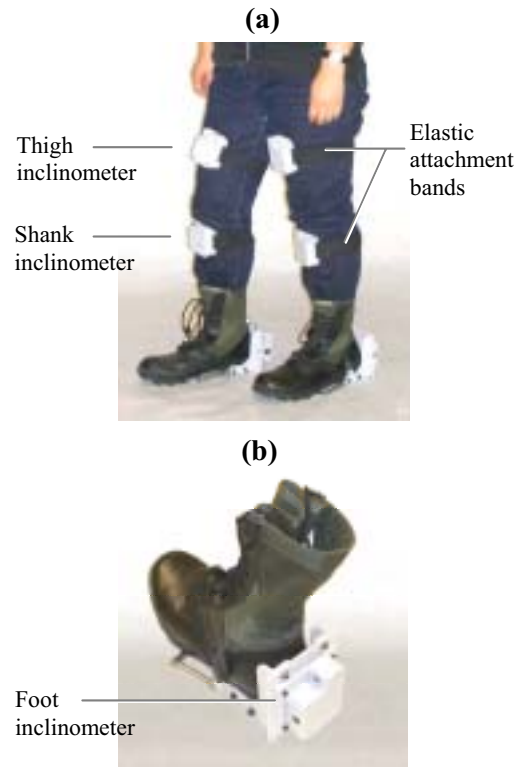Fig. 12. Illustration of flexible contact on torso.

Fig. 13. MicroStrain FAS-G inclinometers used to measure joint angles of human on shank and thigh (a), and foot (b) (connection cables to BLEEX computer not shown).

To prevent the loose harness from impeding the human, the BLEEX controller must be tuned to respond quickly enough in order for the human to not overtake the slack in the harness during rapid maneuvers.

The sensors used to measure joint angles are encoders on BLEEX and inclinometers on the human limbs and torso. An encoder is used on each BLEEX joint to directly measure joint angles in the sagittal plane. BLEEX has two encoders on the ankles, two on the knees, and two on the hips. The human wears inclinometers to measure link angle relative to gravity. In total, seven inclinometers are used with two inclinometers on the feet, two on the shanks, two on the thighs, and one on the torso. Human joint angles are obtained by subtracting the angles between the corresponding proximal and distal links on the human body. Inclinometers were chosen to measure human angles because they are easy to attach to the human and they do not require precise relative alignment between the human's limbs.

The Microstrain FAS-G gyro enhanced inclinometer was selected because of its high resolution (0.1 deg), range of motion (360 deg) and angular velocity range (300 deg/s or 5.24 rad/s). A custom signal amplification board was added to fit the signal to our data acquisition system. The inclinometer and signal amplifying board were repackaged in a custom case. The mounting positions of inclinometers and encoders are illustrated in Figure 13. Elastic straps are used to fasten the inclinometers on the human legs. Since the human foot can move relative to the BLEEX foot and tracking, this small movement is crucial in the toe-off and heel-strike stages, so that inclinometers on the human feet are necessary. The foot inclinometer case is specifically made. It is bolted into the sole of the human shoe and oriented with its sensing axis is parallel to the ankle flexion axis.

In our initial testing, position control was applied to all joints for the entire walking gait cycle (no sensitivity amplification control). It was immediately apparent that the technique was not successful for the swing leg of the single support phase of walking (one foot on the ground). With position control, if the human does not move their torso the master-slave controller keeps the BLEEX torso still. In this case, the human torso and BLEEX torso can be thought of as rigidly bound together. The small freedom of movement remaining in the human toe and heel attachment mechanism is insufficient to allow the human to lift and swing their leg naturally. Thus, with the master-slave controller servoing these angle differences, the overall motion of the human and BLEEX was also unnatural and consequently uncomfortable for the human. For this reason we decided to combine master-slave control with the sensitivity amplification controller.

4.3. Swing Phase: Sensitivity Amplification

The sensitivity amplification controller presented in Kazerooni et al. (2005) needs no direct measurements from the pilot or the human-machine interface (e.g., no force sensors

between the two). Instead, the controller estimates, based on measurements (accelerometers and encoders) from the exoskeleton only, how to move so that the pilot feels very little force. This has been shown to be an effective method of generating locomotion when the contact location between the pilot and the exoskeleton is unknown and unpredictable (i.e., the exoskeleton and the pilot are in contact in variety of places). The basic principle for the control of BLEEX requires a high level of sensitivity in response to the forces and torques imposed by the pilot.

The control of the exoskeleton is motivated below by considering a planar 1 DOF exoskeleton system—a human leg attached or interacting with a 1 DOF exoskeleton leg in a swing configuration (no interaction with the ground). For simplicity, the exoskeleton leg is considered to be a rigid link pivoting about a revolute joint and powered by a single actuator.

Figure 14 shows the control block diagram, where G represents the transfer function from the actuator input, r, to the exoskeleton angular velocity, v (actuator dynamics are included in G). In the case where multiple actuators produce controlled torques on the system, r is the vector of torques imposed on the exoskeleton by the actuators. The sensitivity transfer function, S, represents how the equivalent human torque affects the exoskeleton angular velocity. S maps the equivalent pilot torque, d, onto the exoskeleton velocity, v. The pilot force on the exoskeleton, d, is a function of both the pilot dynamics, H, and the kinematics of the pilot limb (e.g., velocity, position, or a combination thereof). In general, H is determined primarily by the physical properties of the human dynamics. Here we assume H is a nonlinear operator representing the pilot impedance as a function of the pilot kinematics as shown in (4). Many other more detailed models of H also exist (Wilkie 1950; Winters and Stark 1985), but are not necessary for this discussion.

$$d = -H(v) \qquad (4)$$

In Figure 14, H represents human dynamics. Note that for the swing leg because the human and the exoskeleton are tightly connected (since BLEEX torso is controlled by position control), human joint velocities are exactly the same as exoskeleton joint velocities. In contrast, for stance control, as shown in Figure 7, H represents interaction dynamics and the connection between the human and exoskeleton is compliant (i.e., the torso connection is flexible). θ_h and θ_{exo} (i.e., θ_e) are different and this difference is used as the input to the controller.

Positive feedback control is used to achieve our goal of sensitivity amplification:

$$|S_{NEW}| > |S| \quad \forall \omega \in (0, \omega_0) \qquad (5)$$

or alternatively

$$|1 + GC| < 1 \quad \forall \omega \in (0, \omega_0) \qquad (6)$$
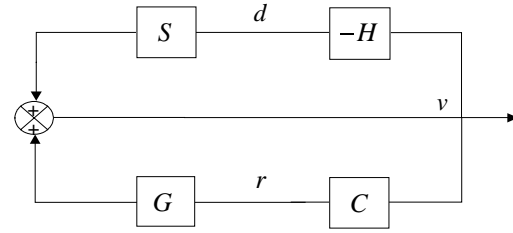

Fig. 14. This block diagram shows how the exoskeleton moves. The upper feedback loop shows how the human moves the exoskeleton through applied forces. The lower feedback loop shows how the controller drives the exoskeleton independent of the human feedback loop.

where ω_0 is the exoskeleton maneuvering bandwidth and S_{NEW} is the closed-loop sensitivity transfer function from human torque, d, at the input to the exoskeleton motion, v, at the output as follows:

$$S_{NEW} = \frac{v}{d} = \frac{S}{1 - GC}. \qquad (7)$$

Exoskeleton control requires a totally opposite goal from classical and modern control theory: *maximize the sensitivity of the closed loop system to forces and torques*. In classical servo problems, negative feedback loops with large gains result in small sensitivity within a bandwidth, which means that they reject forces and torques (usually called disturbances). However, our design goal states that the exoskeleton controller needs a large sensitivity to forces and torques.

To achieve a large sensitivity function, we use the inverse of the exoskeleton dynamics as a positive feedback controller so that the loop gain for the exoskeleton approaches unity (slightly less than 1). In general, the use of positive feedback with a controller is chosen as:

$$C = (1 - \alpha^{-1})G^{-1} \qquad (8)$$

where α is the amplification number greater than unity.

If $\alpha = 10$, then $C = 0.9G^{-1}$, and the new sensitivity transfer function is $S_{NEW} = 10S$ (ten times the force amplification). Equation (8) simply states that a positive feedback controller needs to be chosen as the inverse dynamics of the system dynamics scaled down by $(1 - \alpha^{-1})$. Note that (8) prescribes the controller in the absence of unmodeled high-frequency exoskeleton dynamics. In practice, C also includes a unity gain low pass filter to attenuate the unmodeled high-frequency exoskeleton dynamics that may not be captured in the model, G^{-1}.

The above simple solution comes with an expensive price: robustness to parameter variations. In order to get the above method working, one needs to know the dynamics of the sys-

tem well. When this method is used for all phases of the walking gait cycle, the machine CG, and mass must be known very well. Obtaining a good model of each BLEEX link is not hard since, as the designer, we can control their dimension and construction. However, obtaining a good model of torso is nontrivial because the torso includes a variable payload. In addition, this method is computationally very expensive. In the single stance phase, the controller must calculate the full inverse dynamics of a 7 DOF serial chain of links every time through the control loop. Even on a fast modern microprocessor, this can consume the bulk of the 500 μs computation window corresponding to our 2 KHz control update rate (Kim, Anwar, and Kazerooni 2004). As was shown earlier, the hybrid method allows us to circumvent much of this computation.

To illustrate the sensitivity amplification scheme, experimental results from a 1 DOF sensitivity amplification controller running on the BLEEX hardware are shown in Figure 15. The experiment is run on the left hip of BLEEX. BLEEX is put on jig so that it is in jump mode (both feet are off the ground) and all joint valves are turned off except the left hip to simulate a 1 DOF system. Figure 15 shows the bode plot of hip joint torque tracking as the human moves the BLEEX leg through an angle range similar to the walking gait cycle. The reference torque for the controller is calculated using the sensitivity amplification method. From the bode plot we can see the tracking is acceptable in the low frequency range. With the sensitivity amplification controller and gravity compensation, the human expends little effort to move the BLEEX leg.

4.4. Implementation of the Sensitivity Amplification Controller

In hybrid control, position control is used for the stance leg and a positive feedback sensitivity amplification controller is used for the swing leg. In contrast with the torso, where the unknown and frequently changing payload is located, the swing leg is easier to model accurately. The BLEEX swing leg is modeled as a 3 DOF serial link mechanism in the sagittal plane shown in Figure 16. The dynamics of BLEEX can be written in the general form as:

$$M(\theta)\ddot{\theta} + C(\theta, \dot{\theta})\dot{\theta} + P(\theta) = T + d \qquad (9)$$

where $\theta = [\theta_1 \ \theta_2 \ \theta_3]^T$ and $T = [T_1 \ T_2 \ T_3]^T$.

M is a 3×3 inertia matrix and is a function of θ. $C(\theta, \dot{\theta})$ is a centripetal and Coriolis matrix and is a function of α and $\dot{\theta}$. P is a 3×1 vector of gravitational torques and is a function of θ only. T is the 3×1 actuator torque vector. d is the effective 3×1 torque vector imposed by the pilot on BLEEX at various locations. According to (8), we choose the controller to be the inverse of the BLEEX swing leg dynamics scaled by $(1 - \alpha^{-1})$, where α is the sensitivity amplification gain.

$$T = \hat{P}(\theta) + (1 - \alpha^{-1})\left[\hat{M}(\theta)\ddot{\theta} + \hat{C}(\theta, \dot{\theta})\dot{\theta}\right] \qquad (10)$$

$\hat{C}(\theta, \dot{\theta})$, $\hat{P}(\theta)$ and $\hat{M}(\theta)$ are the estimates of the Coriolis matrix, gravity vector, and the inertia matrix respectively for (9) based on our model of the system. Substituting T from (10) into (9) yields

$$M(\theta)\ddot{\theta} + C(\theta, \dot{\theta})\dot{\theta} + P(\theta) = \hat{P}(\theta)$$
$$+ (1 - \alpha^{-1})\left[\hat{M}(\theta)\ddot{\theta} + \hat{C}(\theta, \dot{\theta})\dot{\theta}\right] + d. \qquad (11)$$

In the limit when $M(\theta) = \hat{M}(\theta)$, $C(\theta, \dot{\theta}) = \hat{C}(\theta, \dot{\theta})$, $P(\theta) = \hat{P}(\theta)$, and α is sufficiently large, d will approach zero, meaning the pilot can swing the leg as if BLEEX did not exist.

5. Transitioning Between Controllers

In the sensitivity amplification controller method proposed in our previous publications, the walking gait cycle is divided into three phases: single support, double support, and double support with one redundancy. The dynamic model is built based on these three phases (Rose and Gamble 1994; Kazerooni et al. 2005). However, in hybrid control, the BLEEX model is based on each individual leg, instead of the status of both legs. Each leg state is decided independently and the corresponding control is implemented.

There are four possibilities for the state of each leg:

Stance: the leg is standing on ground

Swing: the leg is off the ground

Heel-strike: the leg is stepping down to ground

Toe-off: the leg is lifting off the ground

To decide which state each leg is in, two sets of digital pressure activated footswitches are used to provide information about the foot status of each leg. The BLEEX footswitch (Figure 17(a)) is located between the BLEEX foot and ground. When the BLEEX foot is on ground, the BLEEX footswitch is on. The human footswitch (Figure 17 (b)) is located inside the human boot similar to a shoe insole to detect whether the human is attempting to lift their foot. If the human wants to lift the foot, their heel is able to lift up a little inside the boot and this causes the human footswitch to turn off, signaling the controller.

The controller records the foot switch status and keeps track of both the current sample value and the previous sample value. The leg status is decided according to these previous and current footswitch signals. If the previous BLEEX footswitch or human footswitch were off, and currently the BLEEX footswitch and human footswitch are on, then that leg is in the heel-strike mode. If previously both the human footswitch and BLEEX footswitch were on and currently human footswitch or BLEEX footswitch is off (i.e., the human wants to lift up), then that leg is in toe-off mode. If previously the BLEEX and human footswitch were on and currently BLEEX and human footswitch are on, then the leg is in stance mode. If previously the BLEEX or human footswitch
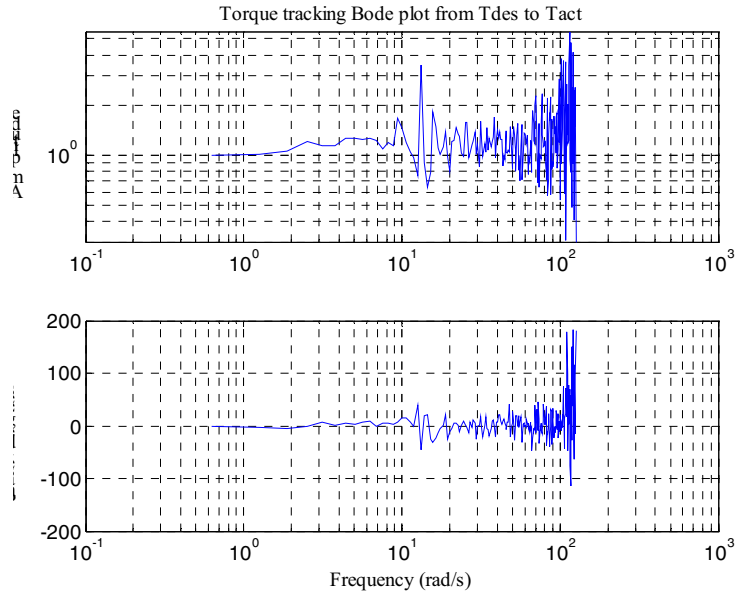
Fig. 15. Bode plot of experimental results from 1 DOF (hip joint) sensitivity amplification controller joint torque tracking.
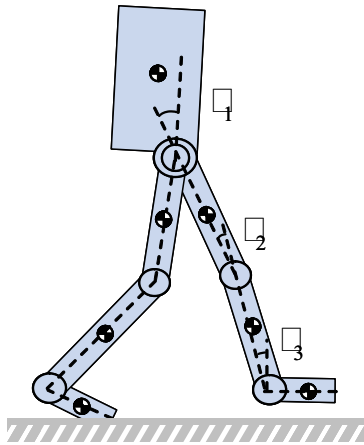

Fig. 16. Sagittal plane representation of BLEEX in the single stance phase (the human pilot is not shown).
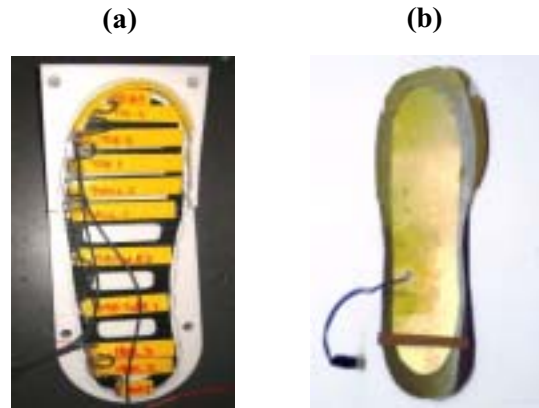

Fig. 17. (a) BLEEX footswitches (between BLEEX and ground) placed in sole mold before being cast in urethane; (b) Human footswitch shoe insole (between BLEEX and human).

were off and currently the BLEEX or human footswitch are off, then the leg is in the swing mode.

5.1. Heel-strike Transition

When stepping down, each joint controller on the leg changes from sensitivity amplification based force control to position control. To prevent the control signal (valve voltage) from undergoing a sudden change, each joint position control gain K gradually changes from a small value, K_s, to the optimum experiment value k_p. Currently this is implemented with a profile function. The transition of the gain is finished in Δt sec. and the current experimental value of Δt is 1 second. This profile function was determined to be most comfortable for the human through experimentation.

5.2. Toe-off Transition

When lifting off ground, each joint controller on the leg changes from position control to force control. Again, to

prevent the control signal from undergoing a sudden change, the implemented actuator torque T in (9) is set to T_{start} (i.e., the actual actuator torques at the beginning of transition), and gradually changed to the calculated value T from (10). As a cost of the smooth transition, the required torque for force control is not completely applied and the human needs to provide extra energy to compensate. Currently this is also implemented with a profile function. The transition of the implemented actuator torque T is finished in Δt sec. and the current experimental value of Δt is 0.4 seconds.

In both heel-strike and stance mode, the same position control algorithm is implemented; only the proportional gain, K, changes. Similarly, in both toe-off mode and swing mode, the same force control is implemented. Only the applied actuator torque, T, changes. For faster walking, the fixed minimum transition period, Δt, will not cause instability but the human will need to provide more energy to achieve the desired motion and speed. Compared with load relief, the extra human energy expenditure was small and considered worthwhile by test subjects. Future work includes adding adaptation algorithms to adjust the two Δt values in response to the walking speed and testing different frequency-domain filtering approaches.

6. Safety Considerations

Because the human is in close contact with the exoskeleton, safety is a very important issue. For the hybrid control scheme, the inclinometers attached to the human are particularly vulnerable. If they were to fail or come loose from the human they could falsely report desired human joint angles that, if the controller were to track, would result in injury or discomfort. To prevent this, if an inclinometer reading error occurs, the controller tracking error $\theta_{hi} - \theta_{exo\,i}$ is software limited to be less than 15 degrees. In addition, if the controller cannot achieve desired tracking performance within a set time window, the system is shut down. These measures help to ensure the controller output will not cause BLEEX to overwhelm the human. Another example of the type of safety considerations that have been added for the hybrid control scheme is to not allow both legs to be in swing simultaneously, which for hybrid control would result in the payload being supported entirely by the human. These safety considerations were added in addition to the extensive safety systems in place on BLEEX for the original sensitivity amplification controller presented in Kazerooni et al. (2005).

7. Discussion

With the hybrid BLEEX control method, a pilot can walk in BLEEX at 0.5 m/s (1.1 mph) with a payload of 18 kg (40 lbs)—tested in a laboratory setting on treadmill. This performance was inferior to the sensitivity amplification controller presented in Kazerooni et al. (2005). Hybrid control does offer other benefits in terms of robustness to changing payload

dynamics. An additional problem encountered while testing hybrid control was that the pilot needed to use a handrail to maintain lateral (side-to-side) balance. Once one leg was in swing, the whole pilot and BLEEX tended to fall toward the swing leg in the lateral plane. This was due in large part to the fact that abduction and adduction joints at the hip were not powered. Because the harness was loosened to improve the performance of the master-slave control mode, the pilot was unable to apply enough torque compensate for the lack of powered hip abduction and adduction. The pilot was able to provide a small balancing torque through the semi-rigid foot connection, but this was insufficient to provide lateral stability. Zoss and Kazerooni (2005) demonstrated that powering the abduction-adduction joints at the hips eliminates the lateral control problem when walking with the sensitivity amplification controller and we conclude that it would also assist in lateral balance for the hybrid control case.

The Berkeley Lower Extremity Exoskeleton (BLEEX) is not a typical servo-mechanism. It requires large sensitivity to pilot forces, which invalidates certain assumptions of the standard control design methodologies. One version of the controller, which we call a sensitivity amplification controller, uses the inverse dynamics of the exoskeleton as a positive feedback so that the loop gain for the exoskeleton approaches unity (slightly less than 1; Kazerooni et al. 2005). The trade off is that this approach requires an accurate model of the system. As an alternative approach, hybrid control is presented. In hybrid control, master-slave control is used for the stance leg and a sensitivity amplification controller is used for the swing leg. In this way, it is not necessary to have a good dynamic model of the torso, which is hard to accurately obtain given that the payload can change. Laboratory walking experiments have been used to demonstrate the feasibility of this method. However, further development is still necessary to improve the inclinometer fastening method, resolve safety issues, and resolve balance issues.

References

Amundsen, K., Raade, J., Harding, N., and Kazerooni, H. 2005. Hybrid Hydraulic-Electric Power Unit for Field and Service Robots. *IEEE Int. Conf. on Intelligent Robots and Systems*, Edmonton, Canada.

Chu, A., Kazerooni, H., and Zoss, A. 2005. On the Biomimetic Design of the Berkeley Lower Extremity Exoskeleton (BLEEX). *IEEE International Conf. on Robotics and Automation*, Barcelona, Spain.

Colombo, G., Jorg, M., and Dietz, V. 2000. Driven Gait Orthosis to do Locomotor Training of Paraplegic Patients. *22nd Annual International Conf. of the IEEE*, EMBS, Chicago, pp. 23–28.

General Electric Co. 1966. Exoskeleton Prototype Project, Final Report of Phase I. General Electric Report S-67-1011, Schenectady, NY.

General Electric Co. 1968. Hardiman I Prototype Project, Special Interim Study. General Electric Report S-68-1060, Schenectady, NY.

Groshaw, P. F. 1969. Hardiman I Arm Test, Hardiman I Prototype. General Electric Report S-70-1019, General Electric Co., Schenectady, NY.

Hirai, K., Hirose, M., Haikawa, Y., and Takenaka, T. 1998. The Development of Honda Humanoid Robot. *Proc. of the 1998 IEEE International Conf. on Robotics & Automation*, Leuven, Belgium, pp. 1321–1326.

Hristic, D. and Vukobratovic, M. 1973. Development of Active Aids for Handicapped. *Proc. of the III International Conf. on Biomedical Engineering*, Sorrento, Italy.

Kawamoto, H., Kanbe, S., and Sankai, Y. 2003. Power Assist Method for HAL-3 Estimating Operator's Intention Based on Motion Information. *Proc. of 2003 IEEE Workshop on Robot and Human Interactive Communication*, Millbrae, CA, pp. 67–72.

Kawamoto, H. and Sankai, Y. 2002. Power Assist System HAL-3 for gait Disorder Person. *International Conf. on Computers Helping People with Special Needs*, Austria.

Kazerooni, H. 1990. Human-Robot Interaction via the Transfer of Power and Information Signals. *IEEE Transactions on Systems and Cybernetics* 20(2):450–463.

Kazerooni, H. 1995. The extender technology at the University of California, Berkeley. *Journal of the Society of Instrument and Control Engineers* 34:291–298.

Kazerooni, H. 1996. The Human Power Amplifier Technology at the University of California, Berkeley. *Journal of Robotics and Autonomous Systems* 19:179–187.

Kazerooni, H. and Guo, J. 1993. Human Extenders. ASME *Journal of Dynamic Systems, Measurements, and Control* 115(2B):281–289.

Kazerooni, H. and Her, M. 1994. The Dynamics and Control of a Haptic Interface Device. IEEE Transactions on Robotics and Automation, 10(4):453–464.

Kazerooni, H. and Mahoney, S. 1991. Dynamics and Control of Robotic Systems Worn By Humans. ASME *Journal of Dynamic Systems, Measurements, and Control* 113(3):379–387.

Kazerooni, H. and Snyder, T. 1995. A Case Study on Dynamics of Haptic Devices: Human Induced Instability in Powered Hand Controllers. *AIAA Journal of Guidance, Control, and Dynamics* 18(1):108–113.

Kazerooni, H., Racine, J.-L., Huang, L., and Steger, R. 2005. On the Control of the Berkeley Lower Extremity Exoskeleton (BLEEX). *IEEE International Conf. on Robotics and Automation*, Barcelona, Spain.

Kim, S., Anwar, G., and Kazerooni, H. 2004. High-speed Communication Network for Controls with Application on the Exoskeleton. *American Control Conference*, Boston, MA.

Kim, S. and Kazerooni, H. 2004. High Speed Ring-based distributed Networked control system For Real-Time Multivariable Applications. *ASME International Mechanical Engineering Congress*, Anaheim, CA.

Kirtley, C. 2005. 10 Young Adults. CGA Normative Gait Database, Hong Kong Polytechnic University. http://guardian.curtin.edu.au/cga/data/

Linskell, J. 2005. Young Adult. CGA Normative Gait Database, Limb Fitting Centre, Dundee, Scotland. Available: http://guardian.curtin.edu.au/cga/data/

Makinson, B. J. 1971. Research and Development Prototype for Machine Augmentation of Human Strength and Endurance, Hardiman I Project. General Electric Report S-71-1056, General Electric Co., Schenectady, NY,

McGee, T., Raade, J., and Kazerooni, H. 2004. Monopropellant-Driven Free Piston Hydraulic Pump for Mobile Robotic Systems. *Journal of Dynamic Systems, Measurement and Control* 126:75–81.

Mizen, N. J. 1965. Preliminary Design for the Shoulders and Arms of a Powered, Exoskeletal Structure. Cornell Aeronautical Laboratory Report VO-1692-V-4.

Mosher, R. S. 1960. Force-Reflecting Electrohydraulic manipulator. *Electro-Technology*.

Mosher, R. S. 1967. Handyman to Hardiman. *SAE Automotive Engineering Congress*. No. 670088, Detroit.

Pratt, J., Krupp, B., Morse, C., and Collins, S. 2004. The RoboKnee: An Exoskeleton for Enhancing Strength and Endurance During Walking. *IEEE Conference on Robotics and Automation*, New Orleans.

Raade, J. and Kazerooni, H. 2004. Analysis and Design of a Novel Power Supply for Mobile Robots. *IEEE International Conference on Robotics and Automation*, New Orleans, LA, pp. 226–232.

Riener, R., Rabuffetti, M., and Frigo, C. 2002. Stair Ascent and Descent at Different Inclinations. *Gait and Posture* 15:32–34.

Rose, J. and Gamble, J. G. 1994. *Human Walking*. Second edition, Williams & Wilkins, Baltimore, p. 26.

Vukobratovic, M., Ciric, V., and Hristic, D. 1972. Contribution to the Study of Active Exoskeletons. *Proceedings of the 5th International Federation of Automatic Control Congress*, Paris.

Wilkie, D. R. 1950. The relation between force and velocity in human muscle. *Journal of Physiology* K110:248–280.

Winter, D.A. 1990. *Biomechanics and Motor Control of Human Movement*. Second edition, Wiley-Interscience, New York.

Winters, J. M. and Stark, L. 1985. Analysis of fundamental human movement patterns through the use on in-depth antagonistic muscle models. *IEEE Trans. on Biomedical Engineering* 32(10):826–839.

Woodson, W., Tillman, B., and Tillman, P. 1992. *Human Factors Design Handbook* New York: McGraw-Hill, pp. 550–552.

Zoss, A. and Kazerooni, H. 2005. On the Mechanical Design of the Berkeley Lower Extremity Exoskeleton. *IEEE Int. Conf. on Intelligent Robots and Systems*, Edmonton, Canada.